DOI 10.1007/s11041-019-00354-w
Metal Science and Heat Treatment, Vol. 60, Nos. 11 – 12, March, 2019 (Russian Original Nos. 11 – 12, November – December, 2018)

UDC 669.715:620.186.1

SYNTHESIS AND INVESTIGATION OF QUATERNARY QUASI-CRYSTALLINE PHASE IN Al – Cu – Fe – Cr ALLOYS

Yifan Wang,[1] Hua Hou,[1] Yuhong Zhao,[1] and Jinzhong Tian[1]

Translated from *Metallovedenie i Termicheskaya Obrabotka Metallov*, No. 12, pp. 17 – 23, December, 2018.

Formation of a quasi-crystalline phase under rapid solidification and heat treatment of alloys of the Al – Cu – Fe – Cr system is studied. The study is performed by x-ray diffractometry, optical, scanning and transmission electron microscopy and differential scanning calorimetry. It is shown that the quasi-crystalline $Al_{65}Cu_{20}Fe_{10}Cr_5$ phase is a mixture of icosahedral and decagonal phases. The substitution of iron with chromium destabilizes the icosahedral *I*-phase and promotes formation of a decagonal *d*-phase. After quenching from 880°C, the $Al_{64}Cu_{24}Fe_{10}Cr_2$ alloy acquires a pure *I*-phase, and the $Al_{64}Cu_{24}Fe_8Cr_4$ alloy acquires a *d*-phase.

Key words: quasicrystalline phase, alloys of the Al – Cu – Fe – Cr system, heat treatment, hardening of melt.

INTRODUCTION

After the discovery of icosahedral quasicrystal formed under rapid solidification of melts of the Al – Mn system [1], quasicrystals have been discovered in alloys of many other systems [2]. In addition to two-component quasicrystals near the Al_6Mn, Al_5Pd and Al_4Ni compositions, quasicrystals have been reported to occur in alloys of the Al – C – Fe, Mg – Zn – Y, and Al – Ni – Si ternary systems [3]. Many aluminum alloys with quasicrystalline phases have found practical application [4]. An icosahedral phase in alloys of the Al – Cu – Fe system with stable and perfect quasicrystalline structure attracts special interest [5].

Several publications have been devoted to the effect of alloying on the stability of ternary icosahedral *I*-phase Al_6Cu_2Fe. However, works on the phase equilibria in quaternary systems with quasicrystalline phases are quite scarce. Some authors assume that quaternary quasicrystals do not exist, and three components are enough for formation of a quasicrystalline phase [6]. According to the data of [7], alloys of the Al – Cu – Fe system acquire ternary compounds and quasicrystalline phases at high cooling rates. However, thin regions of a wedge ingot of the Al – Cu – Fe – Cr quaternary system exhibit a tendency to amorphization [7]. In some cases, substitution of iron with cobalt results in formation of a decagonal phase [8]. Addition of a specific content of a fourth element into the Al – Cu – Fe alloys yields a mixture of icosahedral and decagonal phases [9].

The aim of the present work was to continue the investigation of quasicrystalline phases in alloys of the Al – Cu – Fe and Al – Cu – Fe – Cr systems.

METHODS OF STUDY

We obtained quasicrystalline phases by partial substitution of iron with chromium in alloys subjected to rapid solidification and subsequent heat treatment. The alloys studied had nominal compositions of $Al_{64}Cu_{24}Fe_{10}Cr_2$ and $Al_{64}Cu_{24}Fe_8Cr_4$ prepared from elements with purity 99.99% in an induction furnace in argon atmosphere. The ready melt was poured into a metallic mold.

The microstructure of the alloys was studied with the help of a ZEISS optical microscope, a SU-1500 scanning electron microscope (SEM) equipped with an energy dispersive attachment for chemical analysis, and a JEM2100 transmission electron microscope at an accelerating voltage of 200 kV. The Vickers hardness was measured using a HVS-1000 digital microhardness meter. The x-ray diffraction analysis was performed using a Rigaku D/max-rB diffractometer in copper radiation. The differential scanning calorimetry (DSC) was conducted using a NETZSCH STA 449C device; the powder specimens were heated at a rate of 20 K/min.

[1] College of Materials Science and Engineering, North University of China, Taiyuan, China (e-mail: zhaoyuhong@nuc.edu.cn).

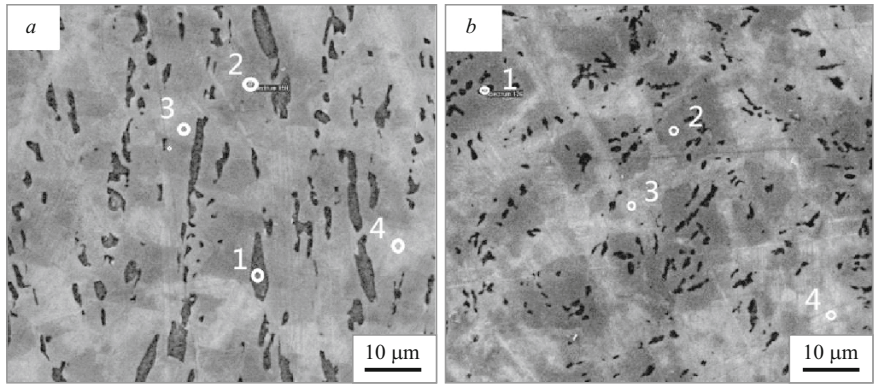

Fig. 1. Microstructure of alloys $Al_{64}Cu_{24}Fe_{10}Cr_2$ (*a*) and $Al_{64}Fe_8Cr_4$ (*b*) in cast condition (SEM): *1*) λ-phase $(Al\text{-}Cu)_{13}Fe_4$; *2*) phase $Al_{65}Cu_{20}Fe_{10}Cr_5$; *3*) *I*-phase $Al_{64}Cu_{24}Fe_{12}$; *4*) η-phase AlCu(Fe).

RESULTS AND DISCUSSION

By the data of the scanning electron microscopy (Fig. 1), both cast alloys $Al_{64}Cu_{24}Fe_{10}Cr_2$ and $Al_{64}Cu_{24}Fe_8Cr_4$ contained four phases, i.e., an $(Al\text{-}Cu)_{13}Fe_4$ λ-phase (colored black), an $Al_{65}Cu_{20}Fe_{10}Cr_5$ phase (dark-gray), an $Al_{64}Cu_{24}Fe_{12}$ *I*-phase (light gray), and an AlCu(Fe) η-phase (white). The compositions of the alloys determined by the energy dispersive analysis are presented in Table 1. The x-ray diffraction patterns in Fig. 2 also show the presence of some Al_2Cu. The light-gray regions correspond to an $Al_{64}Cu_{24}Fe_{12}$ icosahedral quasicrystalline *I*-phase. A similar phase has been described in [10 – 13]. Data on the structure of phase $Al_{65}Cu_{20}Fe_{10}Cr_5$ are quite scarce. We studied it by the method of TEM.

Figure 3*a* presents a gray banded region of alloy $Al_{64}Cu_{24}Fe_{10}Cr_4$, which is represented by phase $Al_{65}Cu_{20}Fe_{10}Cr_5$ with composition $Al_{67.14}Cu_{18.13}Fe_{11.2}Cr_{3.53}$.

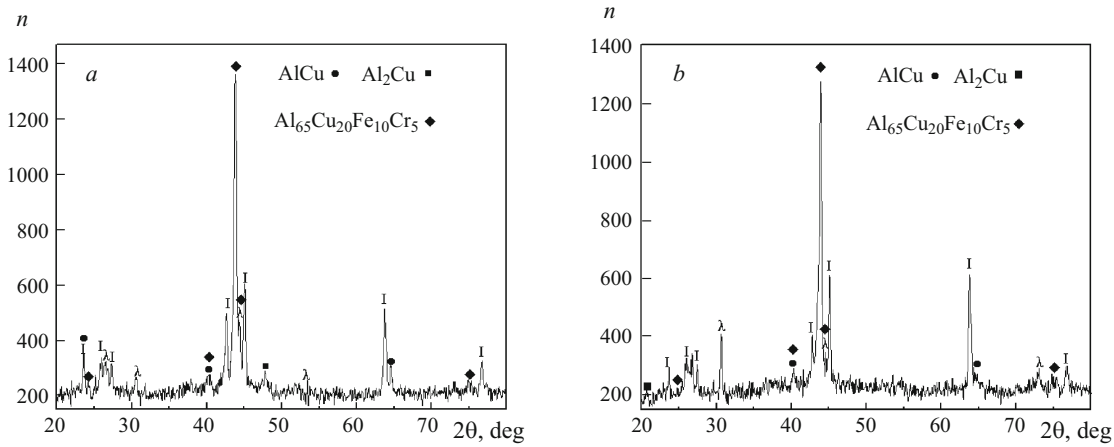

Fig. 2. X-ray diffraction patterns of cast alloys $Al_{64}Cu_{24}Fe_{10}Cr_2$ (*a*) and $Al_{64}Cu_{24}Fe_8Cr_4$ (*b*) (*n* is the number of pulses).

TABLE 1. Chemical Composition of Phases in Alloys $Al_{64}Cu_{24}Fe_{10}Cr_2$ and $Al_{64}Cu_{24}Fe_8Cr_4$ (Fig. 1)

Analyzed point	Phase (color)	Content of elements, at.%				Probable phase
		Al	Cu	Fe	Cr	
1 (Fig. 1*a*)	Black	69.11	6.39	22.32	2.18	$\lambda\text{-}(Al\text{-}Cu)_{13}Fe_4$
2 (Fig. 1*a*)	Dark gray	67.67	15.39	11.56	5.38	(*d* + *I*)-QC
3 (Fig. 1*a*)	Light gray	64.35	24.91	10.74	—	*I*-QC
4 (Fig. 1*a*)	White	53.51	43.66	2.83	–	η-AlCu(Fe)
1 (Fig. 1*b*)	Black	68.54	10.52	17.88	3.06	$\lambda\text{-}(Al\text{-}Cu)_{13}Fe_4$
2 (Fig. 1*b*)	Dark gray	64.21	19.49	11.61	4.70	(*d* + *I*)-QC
3 (Fig. 1*b*)	Light gray	65.71	19.47	14.81	–	*I*-QC
4 (Fig. 1*b*)	White	55.53	40.89	3.58	–	η-AlCu(Fe)

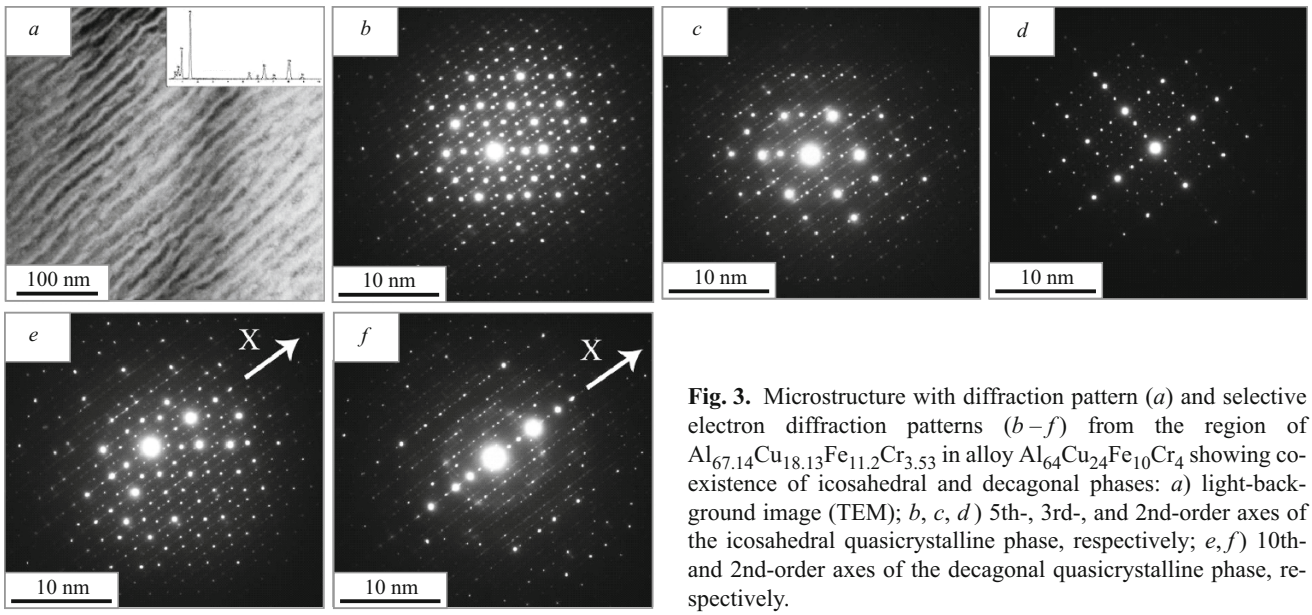

Fig. 3. Microstructure with diffraction pattern (*a*) and selective electron diffraction patterns (*b* – *f*) from the region of $Al_{67.14}Cu_{18.13}Fe_{11.2}Cr_{3.53}$ in alloy $Al_{64}Cu_{24}Fe_{10}Cr_4$ showing coexistence of icosahedral and decagonal phases: *a*) light-background image (TEM); *b*, *c*, *d*) 5th-, 3rd-, and 2nd-order axes of the icosahedral quasicrystalline phase, respectively; *e*, *f*) 10th- and 2nd-order axes of the decagonal quasicrystalline phase, respectively.

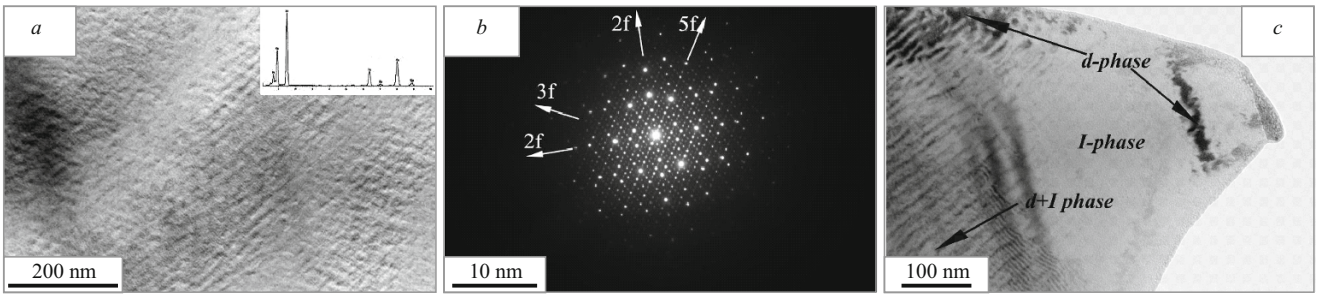

Fig. 4. Structure of *I*-phase (*a*), electron diffraction pattern of the icosahedral quasicrystalline phase showing the 2nd order axis (*b*), and structure of the conjugation (*c*) of the dark-gray (*d*) and light-gray (*I*) phases and their mixture (*d* + *I*) in cast alloy $Al_{64}Cu_{24}Fe_{10}Cr_4$.

It can be seen from Fig. 3*b* – *f* that the $Al_{65}Cu_{20}Fe_{10}Cr_5$ phase contains both quasicrystalline phases, i.e., an icosahedral one and a decagonal one. The electron diffraction patterns in Fig. 3*b* and *d* present the diffraction patterns with quintuple and double symmetry, respectively.

The diffraction pattern in Fig. 3*c* seems to correspond to a third-order symmetry axis of an icosahedral phase. However, we have detected numerous reflections from a rhombic approximant with a great period, which means that the third-order symmetry may be only an approximation. In addition, this region also bears a decagonal quasicrystalline phase, which follows from Fig. 3*e* and *f*. The diffraction pattern in Fig. 3*f* has been obtained upon a turn, which confirms two-dimensional structure of the decagonal quasicrystal. Therefore, as compared to the $Al_{64}Cu_{24}Fe_{12}$ alloy, which consists of only a stable icosahedral *I*-phase, the quasicrystalline phase in the Al – Cu – Fe – Cr alloy should be a mixture of icosahedral and decagonal phases. Exact compositions of these phases are hard to determine.

Figure 4 presents the results of the electron microscopic analysis of the light-gray region *3* (Fig. 1). This region is represented by an *I*-phase. The icosahedral symmetry of the *I*-phase is confirmed by the electron diffraction pattern in Fig. 3*b* with symmetry of the second order. Comparative analysis shows that the homogeneous light-gray region in Fig. 4*a* is an *I*-phase, and the dark-gray phase uniformly alternating with the *I*-phase (Fig. 3*a*) should be a decagonal *d*-phase. This becomes more obvious from Fig. 4*c*, where the arrows point at the *d*-phase, the *I*-phase, and their mixture. In many cases, the *d*-phase and the *I*-phase obey an orientation relation determined in [14]. Thus, the *d*-phase may form from the *I*-phase destabilized by the introduction of chromium, which agrees with the data of [15].

Figure 5 presents the structures of alloys $Al_{64}Cu_{24}Fe_{12}$, $Al_{64}Cu_{24}Fe_{10}Cr_2$ and $Al_{64}Cu_{24}Fe_8Cr_4$ with the indents used to determine the average values of their microhardness, i.e., 790, 692 and 781 *HV*, respectively. It can be seen that the $Al_{65}Cu_{20}Fe_{10}Cr_5$ phase has a microhardness close to that of the icosahedral phase in alloy $Al_{64}Cu_{24}Fe_{12}$, i.e., the replacement of a part of iron with chromium affects little the mechanical properties of the quasicrystalline phase.

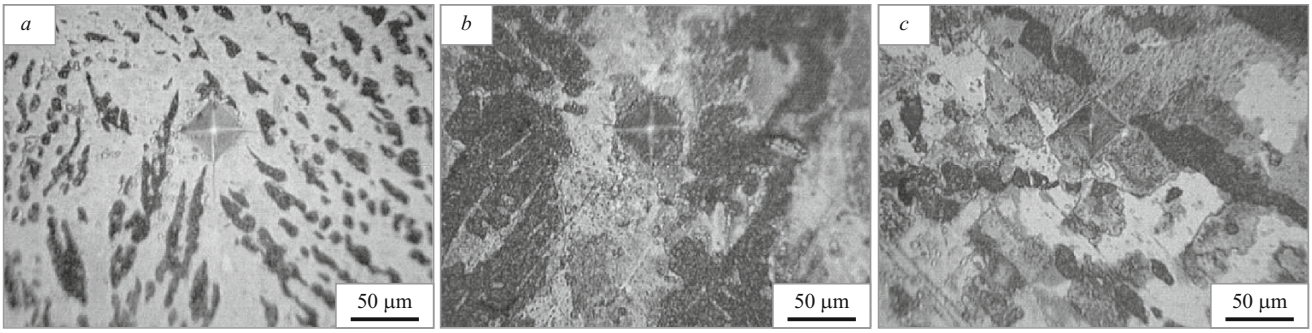

Fig. 5. Structure with indents (at a load of 200 g) obtained due to measuring the microhardness of alloys $Al_{64}Cu_{24}Fe_{12}$ (*a*), $Al_{64}Cu_{24}Fe_{10}Cr_2$ (*b*) and $Al_{64}Cu_{24}Fe_8Cr_4$ (*c*) (optical microscopy).

Figure 6 presents the DSC curves for alloys $Al_{64}Cu_{24}Fe_{12}$, $Al_{64}Cu_{24}Fe_{10}Cr_2$ and $Al_{64}Cu_{24}Fe_8Cr_4$ in heating and cooling at a constant rate of 20 K/min. The peak temperatures are indicated only on the heating curves. The transformations due to heating of alloy $Al_{64}Cu_{24}Fe_{12}$ have been studied in [16 – 18]. This alloy exhibits two successive endothermic effects corresponding to melting of the copper-rich low-melting phase η-AlCu(Fe) (694.85°C) and of the *I*-phase (887.81°C) [17]. The DSC curves of alloys $Al_{64}Cu_{24}Fe_{10}Cr_2$ and $Al_{64}Cu_{24}Fe_8Cr_4$ also exhibit several endothermic peaks and one exothermic peak. Since the quenching from 800°C (6 h) should yield a pure quasicrystalline phase, we studied the effect of heat treatment on the Al – Cu – Fe – Cr alloys. In accordance with the DSC curves, these alloys have a wide endothermic peak at 827°C, which corresponds to melting. The cooling curves exhibit an exothermic peak at 800°C (in the dashed ovals) which should be connected with formation of a phase melting at 827°C. This phenomenon resembles that occurring in the $Al_{64}Cu_{24}Fe_{12}$ alloy. In this connection, we studied the phase transformations in the alloys by the method of x-ray diffractometry. Specimens of cast alloys $Al_{64}Cu_{24}Fe_{10}Cr_2$ and $Al_{64}Cu_{24}Fe_8Cr_4$ were subjected to a hold at 750 and 880°C and then cooled in water and in air.

Figure 7 presents the x-ray diffraction patterns of alloys $Al_{64}Cu_{24}Fe_{10}Cr_2$ and $Al_{64}Cu_{24}Fe_8Cr_4$ after different treatments. The most considerable changes in these curves are disappearance of phase Al_7Cu_2Fe and growth in the content of the quasicrystalline *I*-phase. Therefore, the wide endothermic peak at 827°C may be connected with melting of phase ω-Al_7Cu_2Fe. In addition, in accordance with Fig. 7*a* and *c*, after holding at 880°C and air cooling, Al_7Cu_2Fe becomes one of the main phases, which differs radically from the condition after the hold at 880°C and water quenching. This may be explained by repeated precipitation of the molten Al_7Cu_2Fe phase under slow cooling in air. This agrees with the exothermic peaks near 800°C on the cooling curves of alloys $Al_{64}Cu_{24}Fe_{10}Cr_2$ and $Al_{64}Cu_{24}Fe_8Cr_4$ (Fig. 6). On the whole, quenching from 880°C (30 min) in water provides formation of only quasicrystalline phases (icosahedral and decagonal ones). It should be noted that the intensity of the peaks from phase $Al_{65}Cu_2Fe_{10}Cr_5$ remains high, which indicates its high thermal stability. In addition, the x-ray diffraction patterns of the two alloys reflect the following little difference: phase ω-Al_7Cu_2Fe forms more easily in alloy $Al_{64}Cu_{24}Fe_{10}Cr_2$ at 750°C (Fig. 7).

Figure 8 presents the structure of alloy $Al_{64}Cu_{24}Fe_{10}Cr_2$ after holding at different temperature and cooling in air. It can be seen that phase λ-$(Al\text{-}Cu)_{13}Fe_4$ disappears with growth of the temperature giving place to a gray quasicrystalline phase or an ω-Al_7Cu_2Fe phase. The microstructure of the two alloys after water quenching looks similarly and is not presented in the paper. The composition of the phases (Table 2) in the regions shown in Fig. 9 for alloy $Al_{64}Cu_{24}Fe_{10}Cr_2$ was determined with the help of an energy dispersive attachment to the scanning electron microscope. It turned out (Table 2) that after the heating to 900°C and air cooling phase ω-Al_7Cu_2Fe in region *3* has composition $Al_{68.01}Cu_{21.96}Fe_{10.03}$. However, for the light-gray region *2* the composition is $Al_{64.09}Cu_{26.73}Fe_{9.18}$, which means that the

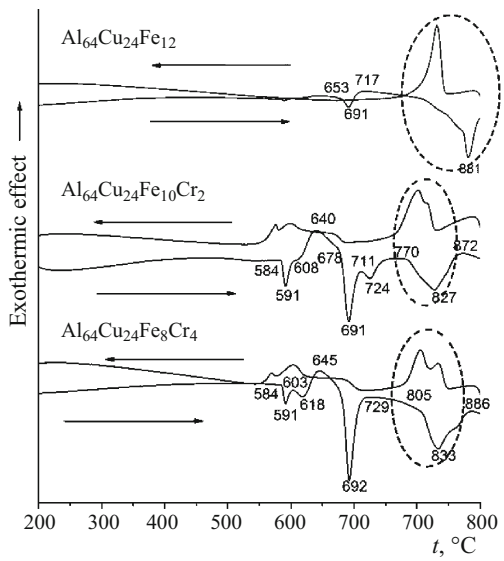

Fig. 6. DSC curves of heating and cooling (indicated by the arrows) at a rate of 20 K/min for alloys $Al_{64}Cu_{24}Fe_{12}$, $Al_{64}Cu_{24}Fe_{10}Cr_2$ and $Al_{64}Cu_{24}Fe_8Cr_4$.

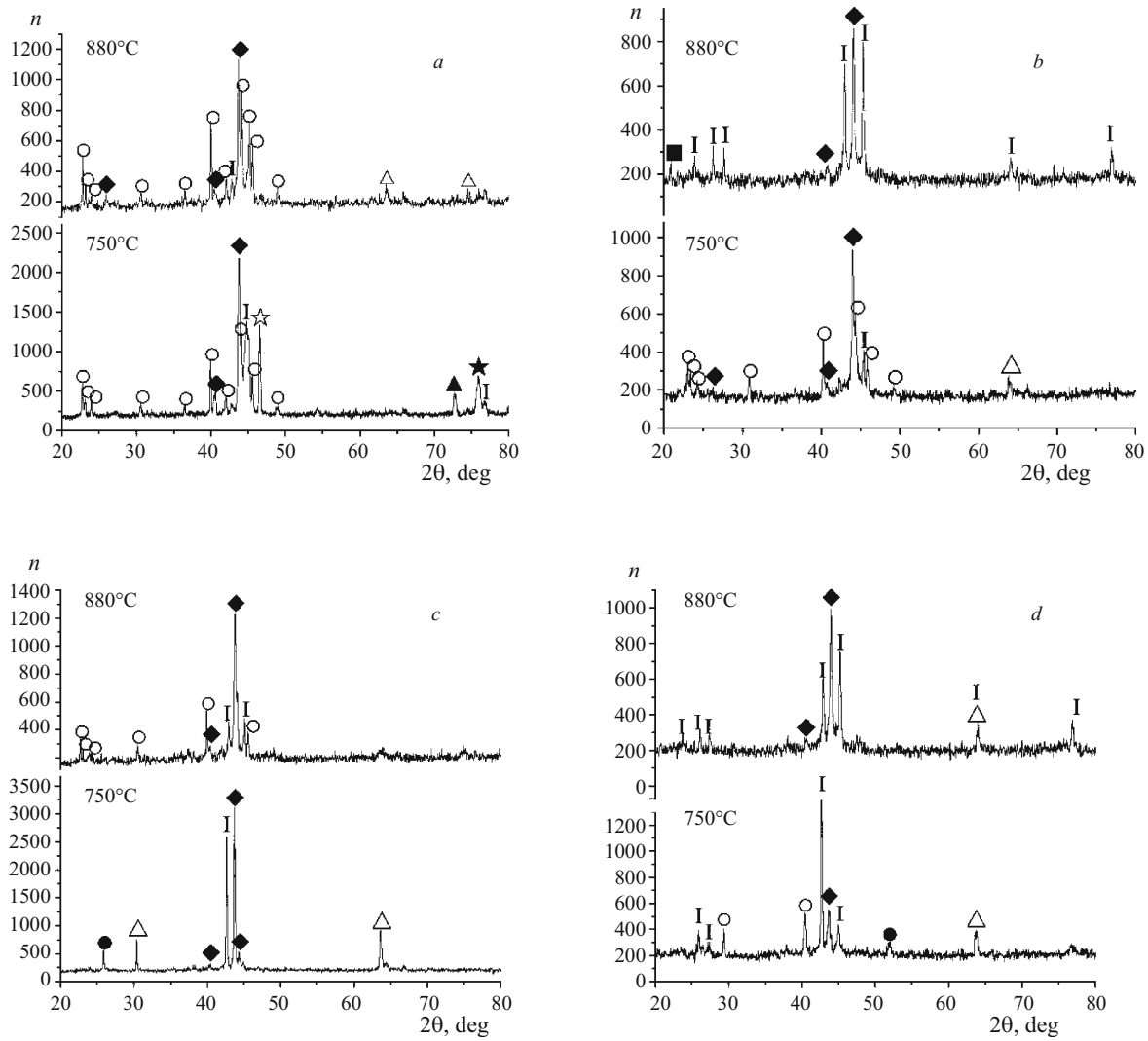

Fig. 7. X-ray diffraction patterns (n is the number of pulses) of alloys $Al_{64}Cu_{24}Fe_{10}Cr_2$ (*a*, *b*) and $Al_{64}Cu_{24}Fe_8Cr_4$ (*c*, *d*) after holding at 750 and 880°C and cooling in air (*a*, *c*) and in water (*b*, *d*): ◆) peaks from $Al_{65}Cu_{20}Fe_{10}Cr_5$; ○) ω-$Al_7Cu_2Fe$; ■) Al_2Cu; ●) AlCu; △) Al_2Cu_3; ▲) $Al_{86}Cr_4$; ★) FeCr; ✯) $AlCu_3$.

I-phase and the ω-Al_7Cu_2Fe phase in this test look approximately similarly. Figure 9*b* presents the $Al_{65}Cu_{20}Fe_{10}Cr_5$ phase and the *I*-phase obtained after water cooling. According to the data of Table 2, the dark-gray region corresponds to phase $Al_{65}Cu_{20}Fe_{10}Cr_5$, and the light-gray region corresponds to the *I*-phase. The uneven region marked with the ar-

TABLE 2. Chemical Compositions of Phases Entering $Al_{64}Cu_{24}Fe_{10}Cr_2$ and $Al_{64}Cu_{24}Fe_8Cr_4$

Analyzed point	Phase (color)	Content of elements, at.%				Probable phase
		Al	Cu	Fe	Cr	
1 (Fig. 9*a*)	Dark gray	65.43	21.57	9.40	3.60	(*d* + *I*)-QC
2 (Fig. 9*a*)	Light gray	64.09	26.73	9.18	–	*I*-QC
3 (Fig. 9*a*)	Light gray	68.01	21.96	10.03	–	ω-Al_7Cu_2Fe
1 (Fig. 9*b*)	Dark gray	61.08	19.73	12.49	6.70	(*d* + *I*)-QC
2 (Fig. 9*b*)	Dark gray	62.32	21.36	12.58	3.74	(*d* + *I*)-QC
3 (Fig. 9*b*)	Light gray	60.28	27.87	11.84	–	*I*-QC

Notations: QC) quasicrystalline phase; *I*) icosahedral phase; *d*) decagonal phase.

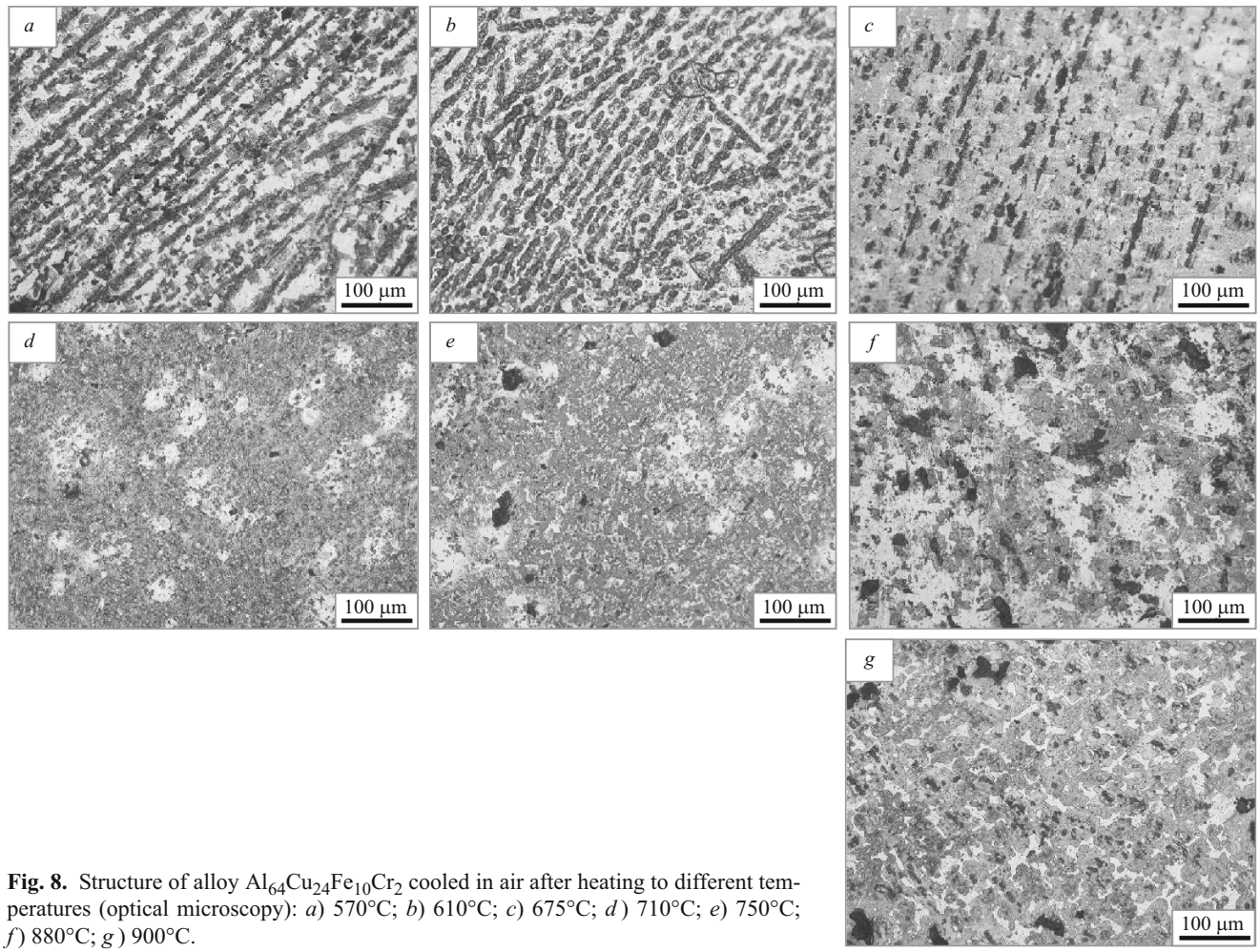

Fig. 8. Structure of alloy $Al_{64}Cu_{24}Fe_{10}Cr_2$ cooled in air after heating to different temperatures (optical microscopy): *a*) 570°C; *b*) 610°C; *c*) 675°C; *d*) 710°C; *e*) 750°C; *f*) 880°C; *g*) 900°C.

row in Fig. 9*b* may be explained by melting of phase λ-$(Al\text{-}Cu)_{13}Fe_4$.

CONCLUSIONS

1. The structure of alloys $Al_{64}Cu_{24}Fe_{10}Cr_2$ and $Al_{64}Cu_{24}Fe_8Cr_4$ in cast conditions contains a quaternary quasicrystalline phase $Al_{65}Cu_{20}Fe_{10}Cr_5$ with rectangular morphology. This phase is a mixture of icosahedral and decagonal quasicrystalline phases. Substitution of iron with chromium destabilizes the icosahedral *I*-phase and stabilizes the decagonal *d*-phase.

2. The studies by the methods of DSC and x-ray diffractometry have shown that heat treatment may produce pure quasicrystalline phases (icosahedral and decagonal ones). When the temperature of the exposure is increased to 880°C, the λ-$(Al\text{-}Cu)_{13}Fe_4$ phase disappears progressively yielding a quasicrystalline *I*-phase and a ω-Al_7Cu_2Fe phase.

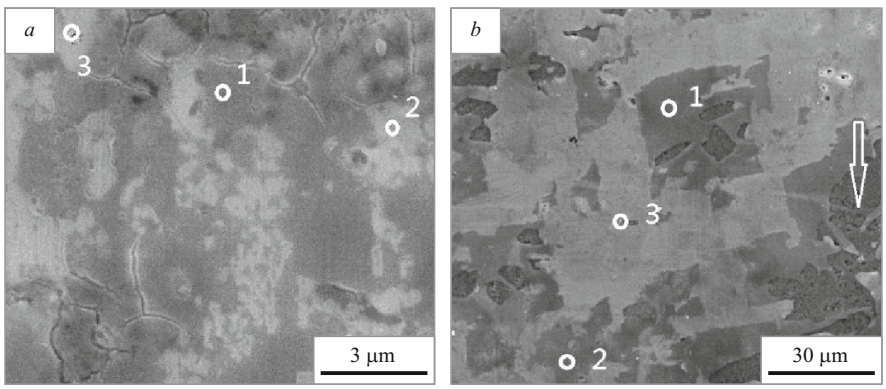

Fig. 9. Microstructure of alloy $Al_{64}Cu_{24}Fe_{10}Cr_2$ after heating to 880°C and cooling in air (*a*) and in water (*b*) (SEM). The description of the phases at points *1 – 3* is given in Table 2.

After the slow air cooling the molten ω-Al_7Cu_2Fe phase precipitates again, while the water quenching yields an *I*-phase.

3. We have detected some differences in the properties and transformations in alloys $Al_{64}Cu_{24}Fe_{10}Cr_2$ and $Al_{64}Cu_{24}Fe_8Cr_4$, i.e., the microhardness of phase $Al_{65}Cu_{20}Fe_{10}Cr_5$ in the $Al_{64}Cu_{24}Fe_8Cr_4$ alloy is higher than in the $Al_{64}Cu_{24}Fe_{10}Cr_2$ alloy; phase ω-Al_7Cu_2Fe forms more easily under heating of the $Al_{64}Cu_{24}Fe_{10}Cr_2$ alloy.

The financial aid from the International Cooperation Project Supported by the Ministry of Science and Technology of China (No. 2014DFA50320), the National Natural Science Foundation of China (No. 51574207, 51574206, 51204147, 51274175), the International Science and Technology Cooperation Project of the Shanxi Province (No. 2015081041) and the Research Project Supported by the Shanxi Scholarship Council of China (No. 2016-Key 2) is gratefully acknowledged.

REFERENCES

1. D. Shechtman, I. Blech, D. Gratias, and J. W. Chan, "Metallic phase with long-range orientational order and no translational symmetry," *Phys. Rev. Lett.*, **53**, 1951 (1984).
2. C. Janot, *Quasicrystals: A Primer*, Oxford University Press (1992).
3. C. Dong, *Quasicrystalline Materials*, National Defense Industry Press, Beijing (1998).
4. M. Feuerbacher, C. Metzmacher, M. Wollgarten, et al., "The plasticity of icosahedral quasicrystals," *Mater. Sci. Eng. A*, **233**, 103 (1997).
5. T. Ishmasa, Y. Fufano, and M. Tsuchimori, "Quasicrystal structure in Al – Cu – Fe annealed alloy," *Philos. Mag. Lett.*, **583**, 157 (1988).
6. C. Dong, J. B. Qiang, Y. M. Wang, et al., "Cluster-based composition rule for stable ternary quasicrystals in Al – (Cu, Pd, Ni) – TM system," *Philos. Mag.*, **86**, 263 – 274 (2006).
7. G. Rosas and R. Perez, "Crystalline and quasicrystalline phases in AlCuFe and AlCuFeCr alloys," *J. Mater. Sci.*, **32**, 2403 (1997).
8. R. Perez, J. A. Juarez-Islas, and J. L. Albarran, "Microstructural characteristics of quasicrystalline phases in alloys of Al – Cu – Fe – Co," *Acta Metall. Mater.*, **40**, 2423 (1992).
9. H. Kim, B. H. Kim, S. M. Lee, et al., "On the phase transitions of the quasicrystalline phases in the Al – Cu – Fe – Co alloy," *J. Alloys Compd.*, **342**, 246 (2002).
10. V. C. Srivastava, E. Huttunen-Saarivirta, C. Cui, et al., "Bulk synthesis by spray forming of Al – Cu – Fe and Al – Cu – Fe-Sn alloys containing a quasicrystalline phase," *J. Alloys Compd.*, **597**, 258 – 268 (2014).
11. C. Patino-Carachure, O. Tellez-Vazquez, and G. Rosas, "XRD and HREM studies from the decomposition of icosahedral AlCuFe single-phase by high-energy ball milling," *J. Alloys Compd.*, **509**, 10036 – 10039 (2011).
12. F. Haidara, B. Duployer, D. Mangelinck, and M.-C. Recorda, "In-situ investigation of the icosahedral Al – Cu – Fe phase formation in thin films," *J. Alloys Compd.*, **534**, 47 – 51 (2012).
13. M. Mitka, A. Goral, L. Rogal, and L. Litynska-Dobrzynska, "Microstructure of mechanically alloyed and annealed $Al_{62}Cu_{25.5}Fe_{12.5}$ powder," *J. Alloys Compd.*, **653**, 47 – 53 (2015).
14. R. J. Schaefer and L. Bendersky, "Replacement of icosahedral Al – Mn by decagonal phase," *Scr. Metall.*, **20**, 745 (1986).
15. C. Dong and J. M. Dubois, "Quasicrystals and crystalline phases in $Al_{65}Cu_{20}Fe_{10}Cr_5$ alloy," *J. Mater. Sci.*, **26**, 1647 – 1654 (1991).
16. S. M. Lee, H. J. Jeon, B. H. Kim, et al., "Solidification sequence of the icosahedral quasicrystal forming Al – Cu – Fe alloys," *Mater. Sci. Eng. A*, **304 – 306**, 871 – 978 (2001).
17. X. P. Li, Z. Xu, and S. Wang, "Preparation of $Al_{63}Cu_{25}Fe_{12}$ powder and phase analysis," *Mater. Rev.*, **17**, 75 – 77 (2003).
18. R. Niculaa, F. Turquier, M. Stir, et al., "Quasicrystal phase formation in Al – Cu – Fe nanopowders during field-activated sintering (FAST)," *J. Alloys Compd.*, **434 – 435**, 319 – 323 (2007).